



## The thermochemical behavior of some binary shape memory alloys by high temperature direct synthesis calorimetry

S.V. Meschel<sup>a,b,\*</sup>, J. Pavlu<sup>c</sup>, P. Nash<sup>b</sup>

<sup>a</sup> James Franck Institute, The University of Chicago, 5640 S. Ellis Avenue, Chicago, IL, 60637, USA

<sup>b</sup> Illinois Institute of Technology, Thermal Processing Technology Center, 10W, 32nd Street, Chicago, IL, 60616, USA

<sup>c</sup> Department of Chemistry, Masaryk University, Kotlarska 2, Brno, 61137, Czech Republic

### ARTICLE INFO

#### Article history:

Received 18 November 2010

Received in revised form 19 January 2011

Accepted 20 January 2011

Available online 5 March 2011

#### Keywords:

Shape memory alloys

Enthalpy of formation

Calorimetry

### ABSTRACT

The standard enthalpies of formation of some shape memory alloys have been measured by high temperature direct synthesis calorimetry at 1373 K. The following results (in kJ/mol of atoms) are reported: CoCr ( $-0.3 \pm 2.9$ ); CuMn ( $-3.7 \pm 3.2$ ); Cu<sub>3</sub>Sn ( $-10.4 \pm 3.1$ ); Fe<sub>2</sub>Tb ( $-5.5 \pm 2.4$ ); Fe<sub>2</sub>Dy ( $-1.6 \pm 2.9$ ); Fe<sub>17</sub>Tb<sub>2</sub> ( $-2.1 \pm 3.1$ ); Fe<sub>17</sub>Dy<sub>2</sub> ( $-5.3 \pm 1.7$ ); FePd<sub>3</sub> ( $-16.0 \pm 2.7$ ); FePt ( $-23.0 \pm 1.9$ ); FePt<sub>3</sub> ( $-20.7 \pm 2.3$ ); NiMn ( $-24.9 \pm 2.6$ ); TiNi ( $-32.7 \pm 1.0$ ); TiPd ( $-60.3 \pm 2.5$ ). The results are compared with some earlier experimental values obtained by calorimetry and by EMF technique. They are also compared with predicted values on the basis of the semi empirical model of Miedema and co-workers and with ab initio calculations when available. We will also assess the available information regarding the structures of these alloys.

© 2011 Elsevier B.V. All rights reserved.

### 1. Introduction

W.J. Buehler and F.E. Wang, two crystal physicists observed in 1959 that NiTi alloy (Nitinol) has unique characteristics [1]. This alloy “remembers” its shape, and therefore such compounds are called shape memory alloys (SMA). Compounds in this group are held in the so called “parent” state, which is usually a cubic structure (Austenite) and heat treated to transform to another structure. When for example the NiTi wire cools below its transition temperature the atoms rearrange in another structure of lower symmetry, the Martensite phase. These are solid state transformations. The Martensite crystals are slightly flexible and can accommodate some degree of deformation. When the NiTi wire is warmed up the Martensite crystals revert to their undeformed, “parent” structure (Austenite). The earliest observations of this effect are credited to Olander in 1932 (Au–Cd), Greeninger and Mooradian (1938) (Cu–Zn) and later to Kurdjumov and Khandros (1949) and also to Chang and Read (1951) [2–5].

The shape memory phenomenon is associated with reversible martensitic transformations [6]. Such transformations may take place either by thermoelastic or by a non-thermoelastic process. When the material is heated up and the structure reverts to the original or “parent phase” it is called a thermoelastic process. How-

ever, there are exceptions, some of the Fe based alloys show a face centered cubic to hexagonal close pack martensitic transformation in a non-thermoelastic way [7,8].

In general, materials which allow structures to adapt to their environment are known as actuators [9]. They can change shape, hardness, position, frequency and other properties as a response to temperature, electricity or magnetism. The thermoelastic shape memory alloys (SMA) may respond to thermal stimuli, piezoelectric ceramics to electric stimuli (PZT = lead zirconate titanate) and magnetostrictive materials to changes of magnetic fields (Terfenol-D, Samfenol, Galfenol) [10]. While this definition is the most general one, we should keep it in mind that though SMA alloys are actuators not all actuators display shape memory phenomenon.

When a SMA recognizes only its “parent” state, it is undergoing a so called “one way” shape memory transition. If the sample undergoes specific “training” treatments, it is possible for the alloy to recognize both its “parent” shape and also its deformed state. The result is the fascinating so called two-way shape memory effect, which is much less well understood [11–14]. This is a unique effect in inanimate materials, however there are similar manifestations in the animal kingdom, for example in the training of homing pigeons.

The shape memory alloys are utilized in many areas of endeavor, including electrical engineering, machinery design, transportation, chemical engineering, space research and medicine. This indicates a great demand for these materials. To 1994 more than 15,000 patents were applied for utilization of SMA-s [13]. These include such diverse specific uses as pipe joints, eyeglass frames, orthodontic treatments, stents in bypass surgeries and many other ingenious applications.

\* Corresponding author at: Illinois Institute of Technology, Thermal Processing Technology Center, 10W, 32nd Street, Chicago, IL, 60616, USA. Tel.: +1 773 684 7795; fax: +1 773 702 4180.

E-mail address: [meschel@jfi.uchicago.edu](mailto:meschel@jfi.uchicago.edu) (S.V. Meschel).

In both the experimental and the theoretical treatments of SMA-s the stability of the alloy is considered very important [15,16]. Since the enthalpies of formation are excellent indicators of the stability of alloys, we believe that understanding the thermochemical behavior of such compounds would be helpful to members of the scientific community who design new shape memory alloys with specific applications in mind [17,18]. We found the list of compounds where shape memory effect has been observed very helpful in identifying the more important shape memory alloys [13,19].

In some instances shape memory effects have been predicted for metallic systems where compound formation has not been reported. Some of the binary alloys which are reported to exhibit shape memory phenomena have only one reported crystal modification. It is questionable if the effect is due to thermoelastic SMA phenomenon if the alloys have no apparent “deformed” modification. We also noticed that in some studies compositions of binary alloys were proposed as exhibiting shape memory effect which are not stoichiometric. Therefore we assessed in the present communication the systems where shape memory effect was reported or predicted and surveyed their basic characteristics. Subsequently we prepared some stoichiometric compositions for detailed thermochemical study.

It is sometimes possible to find information regarding Gibbs' energies or estimate these quantities from phase diagrams, but enthalpies of formation are considerably more scarce. The entropy in these compounds is also a very significant quantity [16]. This quantity plays a crucial role in the transformation of the SMA from the Austenite to the Martensite phase. If the enthalpies of formation are available, it would be possible in principle to evaluate or at least estimate the entropies with existing or estimated Gibbs' energies.

Detailed knowledge of the specific heat could also be very important in understanding the Austenite–Martensite transition. One would anticipate a definite break or discontinuity in the relationship between the specific heat and the temperature at the transition point. Further study of the transition temperature could also advance our understanding of this fascinating process. Rane, Navrotsky and Rossetti studied the detailed thermodynamic behavior of one of the actuators, in a piezoelectric ceramics material (PZT) [10,20].

Therefore we decided to embark on a study of the thermochemical behavior of some SMA-s. In the current communication we are reporting standard enthalpies of formation for some binary SMA-s, namely FePd<sub>3</sub>, FePt, FePt<sub>3</sub>, Fe<sub>2</sub>Tb, Fe<sub>17</sub>Tb<sub>2</sub>, Fe<sub>2</sub>Dy, Fe<sub>17</sub>Dy<sub>2</sub>, NiMn, FeMn, CoCr, Cu<sub>3</sub>Sn and CuMn. Even though the enthalpies of formation for NiTi, TiPd and several Pt alloys have already been measured by high temperature, direct synthesis calorimetry [21,22], we decided to remeasure the enthalpies of formation of NiTi and TiPd, because we felt that the information regarding their structures were not sufficient in the previous studies.

## 2. Experimental

The experiments were carried out at 1373 ± 2 K in a single unit differential calorimeter which has been described in an earlier communication by Kleppa and Topor [23] at the University of Chicago. The measurements in the current study were made at IIT. The changes in the equipment have been reported in an earlier communication [22]. All the experiments were performed under the protective atmosphere of Argon gas which was purified by passing it over titanium chips at 900 °C.

A boron nitride (BN) crucible was used to contain the samples.

All the metals were purchased from Johnson Matthey/Aesar (Ward Hill, MA, USA). The Tb and Dy samples were filed from solid ingots immediately prior to the experiments. For the alloys where we used Fe, Co, Ni or Cu, these were reduced prior to the calorimetric experiments at 600 °C under hydrogen gas flow to insure that we avoid surface oxidation of these metals. The two components were mixed in the appropriate molar ratio, compressed into small pellets of about 2 mm diameter and then dropped from room temperature into the calorimeter. In a subsequent set of experiments the reaction products were dropped into the calorimeter to measure

their heat contents. Between the two sets of experiments the samples were kept in a vacuum desiccator to prevent reaction with oxygen or moisture.

Calibration of the calorimeter was achieved by dropping weighed segments of high purity, 2 mm diameter Cu wire into the calorimeter at 1373 ± 2 K. The enthalpy of pure copper at 1373 K, 43.184 kJ/mol of atoms was obtained from Hultgren et al. [24]. The calibrations were reproducible to within ±2.0–2.5% precision.

The reacted samples were examined by X-ray powder diffraction analyses to assess their structure and to ascertain the absence of unreacted metals. In the course of the present study we attempted to prepare 19 binary alloys. Among these, 14 were found acceptable for fully quantitative measurements. We did not attempt to prepare compositions of binary alloys which were not indicated to exist in the phase diagram collection of Massalski et al. [25]. These are for example alloys in the Ti–Nb, U–Nb, In–Ti and Ti–V systems. We also did not include compounds which had no reported crystal structures either in the ASTM Powder diffraction file or in Pearson's collection of crystallographic data [26], as for example in Ti<sub>3</sub>Ni<sub>4</sub>, Fe<sub>81.6</sub>Ga<sub>18.4</sub>.

The physical characteristics and structures of the binary alloys we prepared are summarized in Table 1. In the second column we list the Chemical Abstracts (CAS) Registry Numbers (RN) of the compounds reported to display shape memory phenomenon. As CA currently indexes over 10 million compounds and alloys, if a compound has no RN assigned to it, it is unlikely to be appropriate for further measurements. In the third column we list the melting points of the compounds and alloys from the data available from the Massalski et al. [25] phase diagram collection. In the fourth column we list the Pearson symbols assigned to the structure of the compound available from the ASTM powder diffraction file and from Pearson's collection of crystallographic data [26]. In order to have a well defined shape memory alloy, both the parent structure and the structure after the transition should be well known. The fifth column designated as comments shows if the reaction was complete and the modification observed in the calorimetric measurements. We did not study the alloys in the systems Ag–Cd and Au–Cd, because the vapor pressure of Cd is such that direct synthesis calorimetry at 1100 °C is not possible. The compounds which we found to be ductile during the preparation could be quite suitable for preparing thin wires and coils.

To prepare the samples for XRD analyses we used an agate mortar and pestle. When this was not sufficient we used a hardened steel die and a hammer. In one case we needed to use a diamond wheel to cut the samples. The alloys we studied varied significantly in behavior, structure characteristics and physical properties. We will discuss some of the more important characteristics in the next section.

## 3. Discussion

### 3.1. Physical properties and structures

#### 3.1.1. Unreacted alloys: RuTa, Ru<sub>2</sub>Ta<sub>3</sub>, Ti<sub>4</sub>Mo<sub>9</sub>

These are all listed as shape memory alloys, however we found that in our conditions they are unreacted. The XRD patterns clearly showed the presence of unreacted elements. In the XRD pattern of Ti<sub>4</sub>Mo<sub>9</sub> we noticed the presence of approximately 20% reaction of the expected compound and two unidentified phases. The XRD equipment is sufficiently sensitive so that we could have observed solid solution formation had there been any.

#### 3.1.2. Fe–Pd system

FePd was ductile and could not be powdered in preparation for XRD analysis. However, we performed an XRD analysis on a very thin pellet and a subsequent SEM study. Both samples show the presence of FePd and a substantial amount of unreacted Fe metal. FePd<sub>3</sub> was also ductile. However, the XRD pattern showed a single phase, a cubic structure. This is the only modification listed in both the ASTM powder diffraction file and Pearson's collection of crystallographic data [26].

#### 3.1.3. Fe–Pt system

Our FePt sample could not be powdered, it yielded only small flakes. However, the XRD pattern showed that this compound is a single phase, a tetragonal structure. This is the only modification listed in the ASTM powder diffraction file and in Pearson's crystallographic data [26,27]. FePt<sub>3</sub> is ductile. We performed an XRD analysis on a very thin pellet and found an excellent match of the published cubic structure. Again, there is only one structure listed [26].

**Table 1**  
Physical properties of some binary shape memory alloys.

Compound	RN	Melting point $T$ ( $^{\circ}\text{C}$ )	Structure Pearson symbol	Comment
NiTi	12035-60-8	1310(c)	cP2, mP4	tP2
Ni <sub>3</sub> Ti	59328-60-8	1380(c)	hP16	
NiTi <sub>2</sub>	108503-16-8	984(p)	cF96	
Ti <sub>3</sub> Ni <sub>4</sub>	105-884	–	–	
TiPd	12165-82-1	1400(c)	cP2, oP4	Both modif.
TiPd <sub>2</sub>	12333-98-1	960(c)	–	
TiPd <sub>3</sub>	12066-72-7	1530(c)	hP16	
Ti <sub>4</sub> Mo <sub>9</sub>	–	–	–	XRD, SEM incomplete
TiNb	12384-42-8	–	–	
TiNb <sub>2</sub>	123188-71-6	–	–	
TiV	–	–	–	
TiV <sub>2</sub>	12067-84-4	–	–	
Ti <sub>2</sub> V	–	–	–	
RuTa	–	1667(p)	oF*	XRD, SEM, unreacted
Ru <sub>2</sub> Ta <sub>3</sub>	–	–	tP2	XRD, SEM unreacted
AgCd	12002-62-9	–	cP2, hP2, cI2, oC4	
Ag <sub>2</sub> Cd	119187-00-7	–	–	
AgCd <sub>2</sub>	276691-61-3	–	–	
AuCd	12044-73-4	629 (c)	oP4, t*4, cP2 hP27, hP18	
InTl	–	–	–	
InTl <sub>2</sub>	–	–	–	
In <sub>2</sub> Tl	–	–	–	
FePd	12022-86-5	790(p) 1304(ordering)	tP4	XRD, SEM Incomplete, ductile
FePd <sub>3</sub>	12310-93-9	820(p) 1304(ordering)	cP4	XRD, single phase ductile, cP4
FePt	12186-46-8	~1300(p)	tP4	XRD, Single phase, tP4
FePt <sub>3</sub>	57679-16-0	~1350(p)	cP4	XRD, single phase Ductile, cP4
Fe <sub>3</sub> Tb	–	1212(p)	hR12	XRD, mixed phase
Fe <sub>2</sub> Tb	12023-38-0452	1187(p)	cF24, hR6	XRD, single phase Both modif.
Fe <sub>17</sub> Tb <sub>2</sub>	12063-75-1	1312(p)	hR19, hP38	XRD, two hexag. modif.
Fe <sub>3</sub> Dy	–	1305(c)	hR12	mixed phase
Fe <sub>2</sub> Dy	12019-81-7	1270(p)	cF24, hR*	s.p., cF24
Fe <sub>17</sub> Dy <sub>2</sub>	12060-29-6	1375(c)	hP38	two hexag. modif.
FeMn	12518-52-4	-(1246 $^{\circ}\text{C}$ , ordering)	cF4, cI2, t**	ductile, tetrag.
Fe <sub>3</sub> Mn	12182-95-5	–	–	
Fe <sub>4</sub> Mn	117443-48-8	–	hP2	
Fe <sub>3</sub> Ga <sub>4</sub>	53237-41-5	906(p)	mc42, t*63	
Fe <sub>3</sub> Ga	12063-30-8	–	hP8, hP2	
FeGa <sub>3</sub>	12062-72-5	824(p)	tP16	
CoCr	12052-27-6	~1283(c)	cI2, cP8	SEM, 90% 1:1
CoCr <sub>2</sub>	159201-78-2	–	–	
Co <sub>3</sub> Cr	15381-39-4	–	hP8	
NiMn	12263-28-4	911(c)	cI2, tP2	tP2
Ni <sub>3</sub> Mn	–	–	cP4	
CuMn	12272-98-9	–	cF4, t*4	Tetrag., ss
Cu <sub>3</sub> Mn	104251-06-1	–	–	
CuGa <sub>2</sub>	68985-62-6	eutectic	tP3	
Cu <sub>11</sub> Ga <sub>39</sub>	–	–	–	
Cu <sub>3</sub> Sn	12019-61-3	676(c)	oC80, cF16, m**	oC80
Cu <sub>6</sub> Sn <sub>5</sub>	12019-69-1	–	hP4, hR22	
Cu <sub>3</sub> Si	12134-36-0	859(c)	hP72, hR*	
Cu <sub>3</sub> Ge	12158-95-1	698(p)	oP8, cI2, hP8, mP4	mP4

### 3.1.4. Fe–Tb and Fe–Dy systems

In both systems the 3:1 compound did not form quantitatively at our conditions. We observed mixed phases where the 1:2 compound was predominant. In both systems the 2:1 compound formed quantitatively. In both 1:2 compounds two modifications are listed, a cubic and a hexagonal phase [26]. In TbFe<sub>2</sub> we observed both modifications. In our sample of Fe<sub>17</sub>Tb<sub>2</sub> the XRD pattern of our sample clearly showed the presence of both the reported hexagonal modifications [26]. There were no indications of unreacted elements or secondary phases. Dy<sub>2</sub>Fe<sub>17</sub> was very difficult to powder. We obtained the sample for the XRD analysis by placing it in a hardened stainless steel die and hammering it 300 times. The structure is a reasonably good match of the hP38 type hexagonal pattern. There were no unreacted elements or secondary phases

present. However, we noticed two unidentified lines in the pattern, which closely matched the hR19 type hexagonal pattern published for Tb<sub>2</sub>Fe<sub>17</sub>. This structure has not been published for Dy<sub>2</sub>Fe<sub>17</sub> [26,28–30].

### 3.1.5. FeMn

This sample is ductile. The XRD performed on a very thin pellet did not match either the Fe or the Mn patterns. Subsequent SEM study showed that the large majority of the sample has a 1:1 composition with a minor component of 1:2 composition [31]. We will show the enthalpy of formation result as indicative.

### 3.1.6. CoCr

This sample did not melt, yielded light grey pellets. The samples are ductile and we could not crush them even in the hardened steel die. The XRD pattern of a very thin pellet did not match the tetragonal CoCr phase. The closest match was with the alpha-Co pattern. A subsequent SEM study showed that our sample was nearly 90% 1:1 composition. The study showed the presence of a few percent of two secondary phases. This alloy has gained considerable current significance by its use in hip joint arthroplasty [32].

### 3.1.7. NiMn

This sample melted, yielded a light grey bead. This alloy sample was very difficult to powder to prepare the XRD samples. We placed it in a hardened stainless steel die and hammered it several hundred times for powder preparation. There are two compounds reported in this system [25], however the XRD patterns are not listed in the ASTM powder diffraction file. We generated the pattern of the 1:1 composition from unit cell parameters and the atomic coordinates of the prototype structure [26]. The XRD pattern showed that we had no unreacted elements or any secondary phases. The experimental pattern closely matched the generated tP2 pattern. Heo et al. report this composition as a solid solution [33].

### 3.1.8. CuMn

This sample melted, and yielded a light grey bead. We could not powder it even in the hardened steel die. We cut the sample with a diamond wheel to prepare for heat content measurements. The XRD pattern showed solid solution formation. The pattern matched closely the tetragonal Mn pattern with significant shift toward the copper peaks [34]. Copper based shape memory alloys were reviewed by Tadaki [8,19].

### 3.1.9. Cu<sub>3</sub>Sn

The samples melted, yielded a light grey bead. This sample could be powdered for XRD analysis. The XRD pattern clearly showed an excellent match of the published orthorhombic structure. There is no evidence for the presence of unreacted elements or secondary phases such as Cu<sub>6</sub>Sn<sub>5</sub>. We observed two extra peaks in the pattern which could possibly be attributed to the cubic modification. The pattern of the cubic modification is not listed in the ASTM powder diffraction file. Therefore we generated this pattern from available unit cell parameters and the appropriate atomic coordinates.

### 3.1.10. TiNi

This sample was a gold toned silvery alloy partially melted, which we could not crush. The sample for XRD analysis was filed from the bead. The XRD pattern showed complete reaction and the CsCl type cubic structure.

### 3.1.11. TiPd

This sample was partially melted, yielded a light grey alloy. Our sample could not be crushed to powder, we were only able to get chips for the XRD analyses.

The XRD pattern showed both the cubic and the orthorhombic modifications.

## 3.2. Standard enthalpies of formation

The standard enthalpies of formation of the shape memory alloys determined in this study were obtained as the difference of two sets of measurements. In the first set the following reaction takes place in the calorimeter:

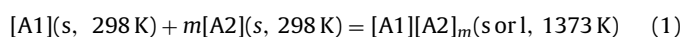


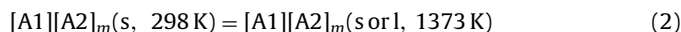
**Table 2**

Standard enthalpies of formation of some binary shape memory alloys. Data are in kJ/mol of atoms.

Compound	$\Delta H(1)$	$\Delta H(2)$	$\Delta H_f^\circ$
FePd <sub>3</sub>	14.4 ± 1.1(5)	30.4 ± 2.5(5)	-16.0 ± 2.7
FePt	6.0 ± 1.5(5)	29.0 ± 1.1(5)	-23.0 ± 1.9
FePt <sub>3</sub>	9.0 ± 1.3(5)	28.7 ± 1.9(4)	-20.7 ± 2.3
Cu <sub>3</sub> Sn	30.1 ± 2.5(6)	40.5 ± 1.8(4)	-10.4 ± 3.1
Fe <sub>2</sub> Tb	25.1 ± 1.6(7)	30.6 ± 1.8(5)	-5.5 ± 2.4
Fe <sub>17</sub> Tb <sub>2</sub>	28.9 ± 2.5(6)	31.0 ± 1.5(5)	-2.1 ± 3.1
DyFe <sub>2</sub>	28.6 ± 2.3(5)	30.2 ± 1.8(5)	-1.6 ± 2.9
Dy <sub>2</sub> Fe <sub>17</sub>	24.0 ± 1.6(5)	29.3 ± 0.7(4)	-5.3 ± 1.7
NiMn	33.0 ± 1.9(4)	57.9 ± 1.8(5)	-24.9 ± 2.6
FeMn <sup>a</sup>	35.7 ± 2.7(6)	38.3 ± 1.6(5)	-2.6 ± 3.1
CoCr	34.3 ± 2.4(5)	34.6 ± 1.7(4)	-0.3 ± 2.9
CuMn	41.1 ± 1.3(5)	44.8 ± 2.9(4)	-3.7 ± 3.2
TiNi	-3.5 ± 0.4(5)	29.2 ± 0.9(5)	-32.7 ± 1.0
TiPd	-29.7 ± 1.8(5)	30.8 ± 1.6(5)	-60.3 ± 2.5

<sup>a</sup> Indicative result.

Here  $m$  represents the molar ratio  $[A1]/[A2]$ , where A1 and A2 represent the elements in the binary shape memory alloys, while  $s$  denotes solid and  $l$  denotes liquid. The reacted pellets were reused in a subsequent set of measurements to determine their heat contents:



The standard enthalpy of formation is given by:

$$\Delta H_f^\circ = \Delta H(1) - \Delta H(2) \quad (3)$$

where  $\Delta H(1)$  and  $\Delta H(2)$  are the enthalpy changes per mole of atoms in the compounds associated with the reactions in Eqs. (1) and (2).

The experimental results are summarized in Table 2. The heat effects associated with the reactions in Eqs. (1) and (2) are given in kilojoules per mole of atoms as averages of about six consecutive measurements with the appropriate standard deviations. The fourth column shows the standard enthalpy of formation of the considered phases. The standard enthalpy of formation in that column also reflects the small contribution from the uncertainties in the calibrations. All the measurements were performed in BN crucibles.

We compared the experimental heat contents of the compounds we studied with the values calculated on the basis of the Neumann-Kopp rule from the heat contents of the elements as listed in Hultgren et al. [24] and found reasonable agreement for most compounds. The average experimental heat content for 14 compounds was  $32.9 \pm 5$  as compared with  $37.9 \pm 3$  kJ/mol of atoms for the calculated values. The experimental and calculated heat contents usually show better agreement when the component metals are all transition metals. We observed some notable deviations for the heat contents of Fe<sub>2</sub>Tb, Fe<sub>17</sub>Tb<sub>2</sub>, FePt, Fe<sub>2</sub>Dy, Fe<sub>17</sub>Dy<sub>2</sub>, FeMn and NiMn where the differences between the experimental and the calculated values are quite substantial. Since NiMn melted under our conditions, some of the difference may be accounted for by the heats of transformation and the heat of fusion.

In Table 3, we compare our results with experimental measurements from the published literature and with predicted values. Some of the enthalpies of formation of the shape memory alloys listed in Table 3 have been measured by Guo and Kleppa [21], by Topor and Kleppa [35] and by Gachon and Hertz [36]. It is noteworthy that our measurement for Cu<sub>3</sub>Sn agrees well with the earlier measurement by Kleppa by tin solution calorimetry in 1957 [37]. We found reasonable agreement for the enthalpy of formation of Dy<sub>2</sub>Fe<sub>17</sub> with Norgren et al. by solution calorimetry [38]. However our result is significantly different for DyFe<sub>2</sub>. The authors refer to errors due to oxidation on p1373 of their study. Also, if we look at the enthalpies of formation of other Fe-LA systems by

**Table 3**

Comparison of the standard enthalpies of formation of some binary shape memory alloys with literature and theoretical predictions. Data are in kJ/mol of atoms.

Compound	Current work	Literature	Method	Prediction Miedema et al. [41] ab initio
NiTi	$-32.7 \pm 1.0$	-34(36) $-33.1 \pm 1.1(20)$	DSC DSC	-52 -33.1
TiNi <sub>3</sub>		-43(36) $-42.2 \pm 1.2(20)$	DSC DSC	-37
NiTi <sub>2</sub>		-29(36)	DSC	-40
TiPd	$-60.3 \pm 2.5$	$-51.6 \pm 6.4(20)$ $-53.3 \pm 1.8(20)$	DSC DSC	-97
TiPd <sub>3</sub>		$-65.0 \pm 0.9(20)$	DSC	-62
FePd <sub>3</sub>	$-16.0 \pm 2.7$	-		-4 -10.0
FePt	$-23.0 \pm 1.9$	$-25(\Delta G) (40)$	EMF	-19 -23.1
FePt <sub>3</sub>	$-20.7 \pm 2.3$	$-17(\Delta G) (40)$	EMF	-11 -19.2
Cu <sub>3</sub> Sn	$-10.4 \pm 3.1$	$-9.1(37)$	SC	-5.4
Fe <sub>2</sub> Tb	$-5.5 \pm 2.4$	-	DSC	-4.4
Fe <sub>17</sub> Tb <sub>2</sub>	$-2.1 \pm 3.1$	$-3.3(39)$	EMF	-1.5
Fe <sub>2</sub> Dy	$-1.6 \pm 2.9$	$-11.1(38)$	SC	-4.4
Fe <sub>17</sub> Dy <sub>2</sub>	$-5.3 \pm 1.7$	$-1.9(38)$ $-4.6(39)$	SC EMF	-1.6
NiMn	$-24.9 \pm 2.6$	-	DSC	-12.3
FeMn	$-2.6 \pm 3.1^a$	-	DSC	+0.4
CoCr	$-0.3 \pm 2.9$	-	DSC	-6.7
CuMn	$-3.7 \pm 3.2$	-	DSC	+5.6

DSC = Direct synthesis calorimetry.

SC = Solution calorimetry.

EMF = Electromotive force measurement.

<sup>a</sup> Indicative result.

different methodologies, the enthalpy values appear to be small, between  $-1$  and  $-5$  kJ/mol of atoms. Therefore the reported value of  $-11.1$  kJ/mol of atoms for DyFe<sub>2</sub> seems unusual. We also found good agreement for the enthalpy of formation of Fe<sub>17</sub>Dy<sub>2</sub> with the measurements of Gozzi et al. [39]. We also found good agreement with the enthalpies of formation for NiTi measured by Gachon et al. by calorimetry [36] and for TiPd measured by Topor and Kleppa [35]. The results of Gozzi et al. and Hultgren et al. were measured by the EMF technique [39,40]. The fourth column indicates the method used in the cited results. The predicted values in the fifth column are from the semi empirical model of Miedema and co-workers [41].

We recently began comparing our results with predicted values by ab initio calculations. This is completely the work of Dr. Pavlu at Masaryk University, Czech Republic and all questions regarding the details of the calculations should be addressed to her. The energies of formation at 0 K temperature were evaluated using the Vienna's Ab initio Simulation Package (VASP), code working within the Density Functional Theory (DFT) [42,43]. This method utilizes the Projector Augmented Wave–Perdew–Burke–Ernzerhof (PAW-PBE) pseudopotentials [44–46]. The Generalized Gradient Approximation (GGA) program was used here to evaluate the exchange correlation energy. The preliminary calculations were accomplished using the experimentally found structural information published in Pearson's collection of crystallographic data and listed in Table 4 [26]. The FePd, FePd<sub>3</sub>, FePt and FePt<sub>3</sub> structures considered here to be ferromagnetic (FM) whereas the NiTi intermetallics in both the cubic and in the monoclinic arrangement are treated as nonmagnetic (NM). The structural parameters for the standard element reference (SER) states: FM bcc Fe, NM fcc Pd and Pt, FM fcc Ni and NM hcp Ti were also cited from [26].

The cut off energy restricting the number of plane waves in the basis set was 348 eV, 326 eV, 299 eV, 350 eV and 232 eV for Fe, Pd, Pt, Ni and Ti respectively, both for pure constituents and constituents in the intermetallic compounds.

We first performed convergence tests of the total energies with respect to the number of k-points. The range of optimum

values extends from a grid of  $23 \times 23 \times 17$  points for FePt, from  $23 \times 23 \times 15$  for FePd, from  $23 \times 23 \times 23$  points for FePd<sub>3</sub> and monoclinic NiTi, to  $31 \times 31 \times 31$  points for FePt<sub>3</sub>, and to  $33 \times 33 \times 33$  points for cubic NiTi.

In the case of the SER structures we used a grid of  $9 \times 9 \times 9$  points for FM bcc Fe and FM fcc Ni, of  $19 \times 19 \times 15$  points for NM hcp Ti, of  $37 \times 37 \times 37$  points for NM fcc Pd and of  $41 \times 41 \times 41$  points for NM fcc Pt. After these calculations, each structure was fully relaxed, which yielded the minimum total energy and the equilibrium structural parameters at 0 K. As the Fe, Pd, Pt and Ni SER structures, FePd<sub>3</sub>, FePt<sub>3</sub> and one of the NiTi modifications are cubic, only the volume relaxation is necessary to obtain their lowest energy state.

The results are summarized in Table 4. The agreement of calculated V/atom with experiments is very good as the deviations of calculated values from experiments (given in % of experimental value) lie in the interval of  $-5\%$ (Pd) to  $+9.5\%$ (Fe) for SER states and in the interval from  $-3.5\%$ (FePd<sub>3</sub>) to  $+4.5\%$ (FePt) for intermetallic phases. The relatively high deviation for pure FM bcc Fe is given by the choice of experimental data. If this deviation is calculated with respect to the second experimental number given in Table 4 its value is only  $+2.3\%$ . The comparison of found and experimental magnetic moments (Table 4) in case of FM bcc Fe, FM fcc Ni, FM FePd, FM FePd<sub>3</sub> and FM FePt provides an excellent agreement. In the case of FePt<sub>3</sub> the antiferromagnetic (AFM) arrangement of the structures is reported [50]. Nevertheless the magnetic moments found in the literature agree very well with the calculated ones.

The above described approach can in principle evaluate the structural stabilities, precise heats of formation, electronic structural properties, chemical bonding, magnetic ordering and defect properties. However, it must be kept in mind that the data rigorously refer to 0 K. Therefore comparison with experimental data at 298 K may give rise to some discrepancies and the ab initio value should be recalculated. In general, the energy of formation of a binary intermetallic compound is obtained as a difference between its equilibrium total energy and the total energies of the

**Table 4**  
Ab initio calculations.

A. Optimized structural parameters of the SER states found in this work and compared with experimental data.					
Structure	a (Å)	b (Å)	c (Å)	$\beta$	V/atom (Å <sup>3</sup> )
FM bcc Fe Exp.	2.9315	a	a	90	12.5962
Exp <sup>a</sup>	2.8576	a	a	90	11.6669
Calc.	2.8358	a	a	90	11.4023
FM fcc Ni Exp.	3.5236	a	a	90	11.0623
Exp. <sup>b</sup>	3.52	a	a	90	10.9036
Calc.	3.5227	a	a	90	10.9286
NM fcc Pd Exp.	3.890	a	a	90	14.7160
Calc.	3.9540	a	a	90	15.4538
NM fcc Pt Exp.	3.923	a	a	90	15.0937
Calc.	3.9772	a	a	90	15.7281
NM hcp Ti Exp.	2.9504	a	4.6810	120	17.6438
Calc.	2.9239	a	4.6249	120	17.1204
B. Optimized structural parameters of the intermetallic compounds found in this work and compared with experimental data. So-called internal parameters of phase describe the positions of atoms within the unit cell and symbols x, y, z denote the axes in the direction of which the position of atoms is defined.					
Structure	a (Å)	b (Å)	c (Å)	$\beta$	V/atom (Å <sup>3</sup> )
FePd exp.	3.8552	a	3.7142	90	13.8006
Calc.	3.8360	a	3.7690	90	13.8649
FePd <sub>3</sub> Exp.	3.8480	a	a	90	14.2444
Calc.	3.8919	a	a	90	14.7378
FePt Exp.	4.0001	a	3.6721	90	14.6891
Calc.	3.8619	a	3.7609	90	14.0230
FePt <sub>3</sub> Exp.	3.8720	a	a	90	14.5126
Calc.	3.9122	a	a	90	14.9692
NiTi Exp.	3.0070	a	a	90	13.5947
Cubic Calc.	3.0047	a	a	90	13.5633
NiTi Exp.	4.6225	4.2105	2.8854	96.8000	13.9409
Monocl.Calc.	4.7812	4.0343	2.9147	102.2351	13.7361
Internal par.	2e – x Ni	2e – z Ni	2e – x Ti	2e – z Ti	
Exp.	0.8070	0.9475	0.2790	0.5274	
Calc.	0.8288	0.9362	0.2851	0.6147	
C. Optimized magnetic moments of the SER states and intermetallic compounds found in this work and compared with experimental data. $\mu$ Denotes average magnetic moment per atom.					
Structure	Ref.	$\mu_{\text{Fe}}$ ( $\mu_{\text{B}}$ )	$\mu_{\text{Ni/Pd/Pt}}$ ( $\mu_{\text{B}}$ )	Comment	
FM bcc Fe	[47] This work	2.12 2.18			
FM fcc Ni	[48] This work		0.61 (Ni) 0.60 (Ni)		
FePd	[49] This work	2.85 2.96	0.35 (Pd) 0.36 (Pd)		
FePd <sub>3</sub>	[49] [49] This work	2.37(13) 3.10 3.30	0.51 (4) (Pd) 0.42 (Pd) 0.35 (Pd)	At 300 K	
FePt	[50] This work	2.8 2.95	0.4 (Pt) 0.35 (Pt)		
FePt <sub>3</sub>	[50] [50] This work	3.3 – 3.26	– 0.38 (Pt) 0.38 (Pt)	AFM arr. FM arr.	
D. Ab initio calculated total energy differences between the intermetallic compound and the weighted averages of total energies of the SER phases of pure constituents. All values are given in kJ/mol of atoms.					
Structure	$\Delta^0 E^{\text{intermet-SER}}$				
FePd	–6.036				
FePd <sub>3</sub>	–10.029				
FePt	–23.095				
FePt <sub>3</sub>	–19.232				
NiTi (cubic)	–33.056				
NiTi (monoclinic)	–37.057				

Å = Angstrom.

1 Å = 0.1 nm.

<sup>a</sup> Ref. [47].<sup>b</sup> Ref. [48].

pure atomic constituents at the same conditions, both calculated ab initio at 0 K. Since in the ab initio calculations the energy per formula unit of the binary compound is evaluated at 0 K there is no entropy contribution. The enthalpy of formation at 0 K is therefore identical with the energy of formation at this temperature and can be calculated at 298 K using Kirchoff's law. Often the approximation of Neumann–Kopp's rule is used and the value of the energy of formation (at 0 K) is approximately compared with the value of the enthalpy of formation (at higher temperatures) without further calculation. The Gibbs' energy of formation is derived from the Gibbs' energy difference of the compound and the pure constituents. It follows that in the derivation of the formation Gibbs' energies it is necessary to know well the Gibbs' energies of the pure phases and include an entropy contribution. The fifth column in Table 3 and part D in Table 4. list the predicted values by ab initio calculations by Dr. Pavlu.

It is encouraging that most of the new predicted values compare quite well with the experimental measurements. Despite some exceptions where we noted discrepancies the agreement is far better than with the Miedema semi empirical model. However, we should keep it in mind that the ab initio calculations refer to 0 K and the experimental measurements to 298 K.

To illustrate the correlations between experimental and predicted values, we have reasonable agreement with the values predicted by the semi empirical model of Miedema and co-workers for 3 alloys from the total of 14 studied. By reasonable agreement our criteria was less than 20% difference between the experimental enthalpies and the predicted values. In comparison, we have reasonable agreement with the values predicted by the ab initio calculations in 3 alloys of the total of 4 for which calculations had been made using the same criteria.

#### 4. Conclusions

- 1 Some aspects of the thermochemical behavior of 14 shape memory alloys are summarized.
- 2 The physical characteristics and the structures of the alloys studied are assessed. Several of the alloys in this study are ductile which is a relevant property in the application of shape memory alloys.
- 3 The standard enthalpies of formation have been measured by high temperature direct synthesis calorimetry.
- 4 The experimental enthalpies of formation were compared with previously determined enthalpies in the published literature and with calculated values from the semi empirical model of Miedema and co-workers and with the ab initio calculations in this work. We found that the ab initio calculations agree better with our experimental measurements.
- 5 The ab initio calculated equilibrium structural parameters and magnetic moments agree very well with those published in the literature. It was shown that the energies of formation corresponding to these equilibrium arrangements can significantly contribute to the analysis of the energetics of intermetallic phases in spite of the fact that they are calculated at 0 K.

#### Acknowledgements

This investigation has benefited from the MRSEC facilities at the University of Chicago and from the facilities in the Thermal Processing Center at IIT. This study was supported by NSF Grant # DMR 0964812 at IIT. Dr. Pavlu's theoretical work was supported by the Grant Agency of the Czech Republic, (Project No.

P108/10/1908), the Ministry of Education of the Czech Republic (Project No. MSM0021622410) and the Academy of Sciences of the Czech Republic (Project No. AV0Z20410507). We would like to express our appreciation to Dr. Ian Steele and to Dr. Joseph Pluth for help with the SEM and the XRD analyses.

#### References

- [1] G.B. Kauffman, I. Mayo, *Chem. Educator* 2 (1997).
- [2] A. Olander, *JACS* 56 (10) (1932) 3819–3833.
- [3] A.B. Greninger, V.G. Mooradian, *Trans. AIME* 128 (1938) 337–355.
- [4] G.V. Kurdjumov, L.G. Khandros, *Doklady Akad. Nauk SSSR* 66 (2) (1949) 211–221.
- [5] L.C. Chang, T.A. Read, *J. Met.* 189 (1951) 47–52.
- [6] K. Otsuka, T. Kakeshita (Eds.), *MRS Bulletin*, Febr. 2002.
- [7] J.H. Yang, H. Chen, C.M. Wayman, *Metall. Trans. A* 23A (1992) 2431–2437.
- [8] K. Otsuka, C.M. Wayman (Eds.), *Shape Memory Materials*, Cambridge University Press, 1998.
- [9] C.A. Rogers, *Sci. Am.* 273 (3) (1995).
- [10] M.V. Rane, A. Navrotsky, G.A. Rossetti Jr., *J. Solid State Chem.* 161 (2001) 402–409.
- [11] J.W. Xie, D. Fort, J.S. Abell, *J. Alloys Compd.* 366 (2004) 241–247.
- [12] R. Stalmans, J. Van Humbeck, L. Delaey, *Acta Metall. Mater.* 40 (1992) 2921–2931.
- [13] M. Freemon, S. Miyazaki, *Shape Memory Alloys*, Springer, New York, 1996, p. 108.
- [14] J. Perkins, D. Hodgson, in: T.W. Duerig, K.N. Melton, D. Stockel, C.M. Wayman (Eds.), *Engineering Aspects of Shape Memory Alloys*, Butterworth-Heinemann, London, 1990.
- [15] I. Muller, S. Seelecke, *Math. Comput. Model.* 34 (2001) 1307–1355.
- [16] I. Friedel, *J. Phys. Lett. (Paris)* 35 (1974) 59–63.
- [17] A.P. Jardine, *J. Mater. Sci.* 24 (1989) 2587–2593.
- [18] J.A. Shaw, Bi-chiau Chang, M.A. Iadicola, Y.M. Leroy, *Proceeding of the SPIE*, 2003, pp. 504976–504987.
- [19] T. Tadaki, K. Otsuka, K. Shimizu, *Ann. Rev. Mater. Sci.* 18 (1988) 25–45.
- [20] G.A. Rossetti Jr., A. Navrotsky, *J. Solid State Chem.* 144 (1999) 188–194.
- [21] Q. Guo, O.J. Kleppa, *J. Alloys Compd.* 321 (2001) 169–182.
- [22] S.V. Meschel, P. Nash, X.Q. Chen, *J. Alloys Compd.* 492 (2010) 105–115.
- [23] O.J. Kleppa, L. Topor, *Thermochim. Acta* 139 (1989) 291–297.
- [24] R. Hultgren, P.D. Desai, D.T. Hawkins, M. Gleiser, D.D. Wagman (Eds.), *Selected Values of the Thermodynamic Properties of the Elements*, ASM, Metals Park, OH, 1973.
- [25] T.B. Massalski, H. Okamoto, P.R. Subramanian, L. Kacprzak (Eds.), *Binary Alloy Phase Diagrams*, 2nd edition, ASM, Metals Park, OH, 1990.
- [26] P. Villars, C.D. Calvert (Eds.), *Pearson's Handbook of Crystallographic Data for Intermetallic Phase*, ASM, Metals Park, OH, 1985.
- [27] Yi-Qun Gao, Zhong-Min Wang, Sung H. Wang, *Materials Sci. Eng. A. Struct. Mater.* A 192–193 (1–2) (1995) 53–58.
- [28] K.N. Martin, P.A.J. de Groot, B.D. Rainford, K. Wang, G.J. Bowden, J.P. Zimmermann, H. Fangohr, *J. Phys. Condens. Matter* 18 (2006) 459–478.
- [29] K.H.J. Buschow, *J. Less Common Met.* 11 (1966) 204–208.
- [30] A.S. Van der Goot, K.H.J. Buschow, *J. Less Common Met.* 21 (1970) 151–157.
- [31] H. Schumann, *Naturwissenschaftliche Reihe* 37 (10) (1988) 47–50.
- [32] A.G. Cobb, T.P. Schmalzreid, *J. Eng. Med. Proc. I. Mech. Eng. Part H* 220 78 (2006) 385–398.
- [33] Y.-U. Heo, M. Kim, H.-C. Lee, *Acta Mater.* 56 (6) (2008) 1306–1314.
- [34] D.P. Oxley, R.S. Tebble, K.C. Williams, *J. Appl. Phys.* 34 (4) (1963) 1362–1364.
- [35] L. Topor, O.J. Kleppa, *Z. Metallkunde* 77 (1986) 633–636.
- [36] J.C. Gachon, J. Hertz, *CALPHAD* 7 (1983) 1–12.
- [37] O.J. Kleppa, *J. Phys. Chem.* 60 (1956) 852–858.
- [38] S. Norgren, F. Hodaj, P. Azay, C. Colinet, *Metall. Mater. Trans.* 29A (1998) 1367–1374.
- [39] D. Gozzi, M. Iervolino, A. Latini, *J. Chem. Eng. Data* 52 (2007) 2350–2358.
- [40] R. Hultgren, P.D. Desai, D.T. Hawkins, M. Gleiser, K.K. Kelley, *Selected Values of the Thermodynamic Properties of Binary Alloys*, ASM, Metals Park, OH, 1973.
- [41] F.R. deBoer, R. Boom, W.C.M. Mattens, A.R. Miedema, A.K. Niessen, *Cohesion in Metals. Transition Metal Alloys*, Elsevier Sci. Publ., The Netherlands, 1988.
- [42] G. Kresse, J. Furthmuller, *Comput. Mater. Sci.* 6 (1) (1996) 15–50.
- [43] G. Kresse, J. Furthmuller, *Phys. Rev.*, B 54 (16) (1996) 11169–11186.
- [44] P. Blochl, *Phys. Rev.*, B 50 (24) (1994) 17953–17979.
- [45] G. Kresse, J. Joubert, *Phys. Rev. B* 59 (3) (1999) 1758–1775.
- [46] J.P. Perdew, K. Burke, M. Ernzerhof, *Phys. Rev. Lett.* 77 (18) (1996) 3865–3868.
- [47] E.G. Moroni, T. Jarlborg, *Phys. Rev. B* 47 (6) (1993) 3255–3267.
- [48] E.G. Moroni, G. Kresse, J. Hafner, J. Furthmuller, *Phys. Rev. B* 56 (24) (1997) 15629–15645.
- [49] H.P.J. Wijn (Ed.), *Magnetic Properties of Metals d-Elements, Alloys and Compounds*, Springer-Verlag, Berlin Heidelberg, Germany, 1991.
- [50] K.H.J. Buschow (Ed.), *Handbook of Magnetic Materials*, Elsevier Sci. B.V., Amsterdam, The Netherlands, 2001.